Iranian Journal of Basic Medical Sciences
ijbms.mums.ac.ir

Delta opioid peptide (D-Ala2, D-Leu5)-enkephalin (DADLE) mitigates myocardial ischemia-reperfusion injury by inhibiting the TRAF6/NF-κB/NLRP3 pathway

Linwen Liu [1], Yawu Sun [1], Yinyan Wu [2], Yang Wang [3], Wei Chen [1]*

[1] Department of Cardiology, Shanghai Fourth People's Hospital Affiliated to Tongji University, Shanghai, China
[2] Department of Neurology, Shanghai Fourth People's Hospital Affiliated to Tongji University, Shanghai, China
[3] Department of Pathology, Shanghai Fourth People's Hospital Affiliated to Tongji University, Shanghai, China

ARTICLE INFO

Article type:
Original

Article history:
Received: Apr 27, 2025
Accepted: Nov 1, 2025

Keywords:
Delta
Myocardial reperfusion injury
NF-kappa B
NLRP3 protein
Opioid
Receptor
TNF receptor-associated factor 6

ABSTRACT

Objective(s): This study aimed to assess the dose-dependent effect of DADLE and to explore its relationship with the TRAF6/NF-κB/NLRP3 pathway.

Materials and Methods: After 45 min of ischemia, reperfusion was sustained for 24 hr in mice to establish the myocardial infarction model. DADLE was administered at doses of 0.25, 0.5, or 1 mg/kg to this model. TTC-Evans Blue double staining, HE staining, and Masson staining were conducted to evaluate myocardial injury. TUNEL staining was used to detect apoptosis. Western blotting and immunofluorescence staining were applied to measure levels of TRAF6, NF-κB p65, NLRP3, caspase-1, pro-caspase-1, and ASC. ELISA assays were used to assess TNF-α and IL-1β levels.

Results: DADLE at all three doses lessened the infarcted area compared with the PBS control. DADLE at 0.5 mg/kg was more efficacious than 0.25 and 1 mg/kg in reducing the infarcted size, pathological scores, and fibrosis. DADLE effectively reduced the number of apoptotic cells as shown by the TUNEL assay. Levels of TRAF6, NF-κB p65, ASC, NLRP3, caspase-1, and pro-caspase-1 proteins were increased after ischemia-reperfusion (I/R) but were reversed by DADLE. Immunofluorescence staining results for NF-κB and NLRP3 demonstrated similar changes. ELISA assays showed that TNF-α and IL-1β concentrations were increased in the model and reversed by DADLE.

Conclusion: DADLE can significantly ameliorate myocardia ischemia-reperfusion injury (MIRI), with the dosage of 0.5 mg/kg presenting the greatest benefit. DADLE may exert its protective effects by activating the TRAF6/NF-κB/NLRP3 signaling pathway.

▶ Please cite this article as:
Liu L, Sun Y, Wu Y, Wang Y, Chen W. Delta opioid peptide (D-Ala2, D-Leu5)-enkephalin (DADLE) mitigates myocardial ischemia-reperfusion injury by inhibiting the TRAF6/NF-κB/NLRP3 pathway. Iran J Basic Med Sci 2026; 29: 218-224. doi: https://dx.doi.org/10.22038/ijbms.2025.87794.18971

Introduction

Coronary atherosclerotic heart disease (CHD) remains the leading cause of mortality globally (1). In recent years, the mortality rate related to acute myocardial infarction (AMI) has been increasing (2). Although coronary reperfusion therapies rescue endangered myocardial cells, the restoration of blood flow paradoxically aggravates ischemic injury, resulting in reperfusion arrhythmia, myocardial dysfunction, and even death (3, 4). Since myocardial ischemia-reperfusion injury (MIRI) undermines the benefit of restoring coronary artery blood flow, effective strategies to alleviate MIRI are urgently needed.

Opioid receptors, including μ (mu), κ (kappa), and δ (delta), play critical roles in regulating the physiological functions of myocardial cells **(5)**. DADLE is a synthetic agonist specifically targeting the δ opioid receptor (DOR) **(6)**. Our research group has extensively studied DADLE's protective role against ischemia-reperfusion injury (IRI) and its underlying mechanisms. Our previous study revealed that DADLE significantly alleviated myocardial injury and enhanced cardiac functions in mice by down-regulating the Wnt/β-catenin pathway through various experimental methods (7). However, the dose-effect relationship and mechanisms through which DADLE mitigates MIRI remain incompletely understood. The protective mechanisms of DOR agonists in IRI include suppression of apoptosis, inhibition of oxidative stress, and attenuation of inflammatory responses (8, 9). We have previously confirmed that DADLE mitigates inflammation through down-regulating the TLR4/NF-κB pathway in the brain (10). NF-κB, triggered by multiple inflammatory cascades during reperfusion, induces overexpression of proinflammatory chemokines and cytokines, including IL-1β and TNF-α, which amplify the inflammatory response and eventually exacerbate MIRI (11, 12). TRAF6, a critical signal transducer, is mainly involved in classical NF-κB signaling activated by TLR and IL-1 (13, 14). Whether DADLE's cardioprotective effects involve the TRAF6/NF-κB pathway remains to be determined.

The progression of MIRI has been shown to be closely associated with pyroptosis, a recently characterized mechanism of programmed inflammatory cell death. (15). The classical pyroptosis pathway depends on caspase-1 activation, which is initiated by the formation of the

***Corresponding author:** Wei Chen. 1279 Sanmen Road, Hongkou District, Shanghai 200434, China. Tel: 8618917684083, Email: 18917684083@189.cn

inflammasome complex. This complex consists of NLRP3, apoptosis-associated speck-like protein with a caspase recruitment domain (ASC), and pro-caspase-1 (16). Upon activation, pro-caspase-1 is cleaved to form the active enzyme, caspase-1, which facilitates the secretion of downstream cytokines, such as IL-1β (17). Studies have demonstrated that inhibiting pyroptosis can significantly mitigate MIRI (18-20). Targeting pyroptosis represents a promising therapeutic strategy to mitigate inflammation and myocardial injury (21).

In this study, we investigated the dose-dependent effects of DADLE on MIRI and explored its underlying mechanisms, including its ability to mitigate MIRI via the TRAF6/NF-κB/NLRP3 signaling pathway. The findings of this study aim to provide novel therapeutic strategies for improving patient outcomes in myocardial infarction (MI).

Materials and Methods

Reagents

DADLE, antibodies against NF-κB p65, TRAF6, pro-caspase-1, NLRP3, caspase-1, and ASC were all obtained from Abcam Biotechnology (Cambridge, MA, USA). Evans blue and TTC were bought from Beyotime Biotechnology (Shanghai, China). Secondary antibodies were acquired from Share Biotechnology (Shanghai, China). TNF-α and IL-1β ELISA kits were purchased from Enzyme Immunoassay Biotechnology (Wuhan, Hunan, China). The TUNEL assay kit was purchased from Beyotime Biotechnology (Shanghai, China).

Animal and ethics statement

C57BL/6J mice, weighing between 22 and 26 g, were obtained from Ziyuan Experimental Animal Technology in Hangzhou, Zhejiang, China. Upon arrival, the mice were acclimated in a regulated environment with a consistent temperature and relative humidity. The mice were provided with unrestricted access to food and water. The Ethics Committee of Shanghai Tongji University approved all experimental procedures (Approval No. TJBH02121201).

Administration of drugs in individual groups

Fifty mice were randomly assigned numbers, and their weights were recorded. A computer randomized method was used to divide the mice into five groups: a sham group, a PBS control group (n = 10), the D1 group (DADLE at 0.25 mg/kg, n = 10), the D2 group (DADLE at 0.5 mg/kg, n = 10), and the D3 group (DADLE at 1 mg/kg, n = 10). DADLE was prepared in PBS for all dosing regimens. During the ischemic phase, 5 min before reperfusion, either PBS or the specified dose of DADLE was administered intraperitoneally. The surgical procedure in the sham group was identical, except that the LAD of the mice was not ligated. Both the control and sham groups were given PBS of equal volumes according to the same administration protocol as the DADLE groups. The summary of the experimental procedures is presented in Figure 1A.

Myocardia ischemia-reperfusion (MI/R) modeling

The experimental model is identical to our previous one (7), refined from the classic model (22). Mice were adequately sedated using 5% isoflurane. Myocardial ischemia was then induced via a left thoracic incision to expose the heart, followed by occlusion of the LAD. After 45 min of ischemia, the LAD ligation was loosened, and reperfusion was maintained for 24 hr. The sham group went through the same surgical procedure without LAD occlusion. Twenty-four hours after MI/R induction, heart tissue samples were collected for subsequent experiments.

HE staining and Masson trichrome staining

Heart tissue samples were dissected and fixed in formalin. These samples were then dehydrated and embedded in paraffin. 5-μm-thick sections were sliced and mounted on glass slides. H&E and Masson staining were performed by following the protocol. Morphological characteristics were subsequently analyzed, and representative images were captured with a bright-field microscope.

Pathological evaluation of each heart section was performed according to our previous scoring system, based on the classic one (23): zero = no injury; one = focal injury; two = multiple injury with minor inflammation, with occasional disorganization of myocardial fibers; three = extensive myofibrillar necrosis and/or inflammation, where moderate damage and fracture of fibers are observed, and four = necrocytosis with wide inflammation, where myocardium show extensive damage, accompanied by

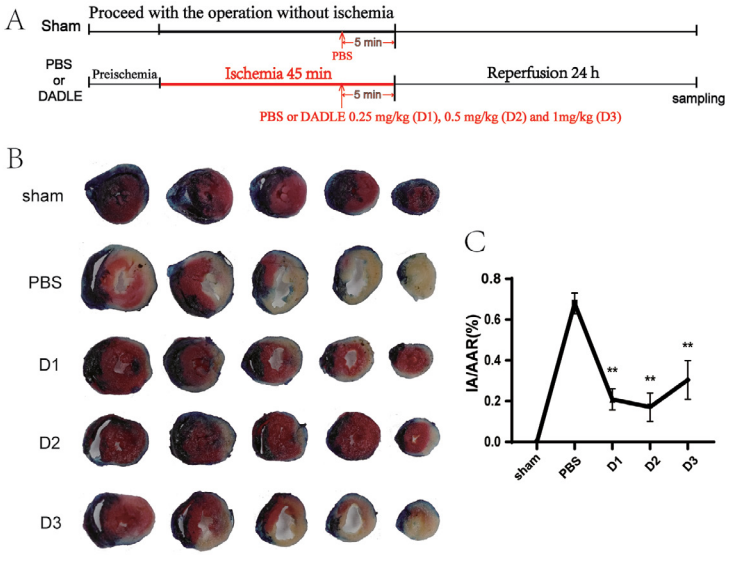

Figure 1. DADLE of different doses significantly decreased the cardiac infarct area in C57BL/6J mice

(A) Schematic diagram depicting the experimental procedures. (B) Typical pictures of 2,3,5-triphenyl tetrazolium chloride (TTC)-Evans blue staining in the sham, PBS control, D1 (0.25mg/kg), D2 (0.5mg/kg), and D3(1mg/kg) groups following myocardia ischemia-reperfusion (MI/R). (C) Ischemic area (IA) /area at risk (AAR) (%). Results are presented

widespread inflammation, and significant disorganization of myocardial fibers. For each slide, three random visual fields of the ischemic region were selected, and pathology scores were assigned. The analysis was conducted by two independent observers unaware of the experimental protocol.

TTC-Evans blue double staining

After 24 hr of I/R treatment, again LAD was ligated. Evans blue solution was infused into the heart. Subsequently, the heart sample was dissected and sliced into 2 mm-thick sections. The slices were then treated with TTC for 15 min. The devitalized tissue was stained white, while the viable myocardium turned brick-red. Non-ischemic areas appeared blue. Both areas at risk of ischemia (AAR, white and brick-red) and the ischemic area (IA, white) were pictured and analyzed using ImageJ. The ratio of IA to AAR (%) was applied to assess alterations of the infarct area.

Western blot

Proteins were extracted from heart tissue, separated by SDS-PAGE, and subsequently transferred to a PVDF membrane. The membrane was incubated with primary antibodies targeting NF-κB p65, TRAF6, NLRP3, ASC, caspase-1, pro-caspase-1, and GAPDH at 4 ℃ for 16 hr. Following this, the membrane was washed and incubated with appropriate secondary antibodies at room temperature for 1 hr. The protein bands were detected using an enhanced chemiluminescence (ECL) system for visualization. Quantitative analysis of the blots was performed using ImageJ.

TUNEL staining

Apoptosis was assessed using a TUNEL assay kit following the manufacturer's instructions. In the fluorescence images, TUNEL-positive nuclei appeared green. The percentage of TUNEL-positive cells was calculated from the captured images.

Immunofluorescent staining

The embedded paraffin sections were dewaxed and subjected to antigen retrieval. Non-specific binding sites were then blocked using bovine serum albumin. The slices were incubated separately with a goat anti-NLRP3 antibody and a Rabbit anti-NF-κB antibody at 4 ℃ overnight, followed by incubation with a Goat anti-rabbit IgG (H+L) cross-adapted secondary antibody at 37 ℃ for 30 min. Finally, they were counterstained with DAPI in the dark. Visualization was performed using a fluorescence microscope. The relative fluorescence intensity was analyzed using ImageJ.

ELISA

Blood samples were drawn from the ocular artery in the mouse. After centrifugation, the supernatant was gathered. The concentrations of serum TNF-α and IL-1β were assessed using ELISA kits according to the manufacturer's protocols.

Statistical analysis

Data were analyzed using SPSS 26. Statistical significance was evaluated using one-way ANOVA or Student's t-test. All figures were presented as mean ± SD. A *P*-value below 0.05 indicates statistical significance.

Results

DADLE at different doses mitigated MIRI in mice

TTC-Evans blue double staining and HE staining were utilized to evaluate the extent of MIRI following DADLE administration. TTC-Evans blue double staining demonstrated infarcted areas (Figure 1B). All three doses of DADLE significantly reduced the infarct size ($P<0.01$). As shown in Figures 1C and 1D, DADLE at 0.5 mg/kg (D2 group) reduced infarct size compared to 0.25 mg/kg (D1 group); however, increasing the dose to 1 mg/kg (D3 group) did not result in a further reduction.

Representative pathological photographs of the myocardium in the ischemic region at lower magnification are exhibited in Figure 2A-E. Representative HE photographs of ischemic cardiomyocytes at higher magnification are shown in Figure 2F-J. As indicated in Figure 2K, similar to the trend in Figure 1C, increasing the dosage from 0.25 mg/kg (D1 group) to 0.5 mg/kg (D2 group) reduced the pathological score ($P<0.01$), but further increasing the dose did not provide additional benefit.

Masson staining was applied to determine fibrosis. As illustrated in Figure 2L-P, DADLE effectively reduced fibrosis during the early stage of cardiac remodeling, demonstrating a trend similar to the pathological changes.

DADLE inhibited the activation of the NF-κB pathway induced by MI/R

The effect of DADLE on the NF-**κB** pathway was assessed via western blot and ELISA. After experiencing I/R, NF-κB p65 expression increased in the PBS group, as shown by Western blot (Figure 3). DADLE at both doses of 0.25 and 0.5 mg/kg significantly reversed NF-κB p65 expression observed in model mice (both $P<0.01$). TRAF6 expression also decreased with DADLE treatment compared with the PBS control group, with a more pronounced reduction observed in the D2 group ($P<0.01$) than the D1 group ($P<0.05$).

ELISA data presented significantly elevated levels of inflammatory mediators (TNF-α and IL-1β) in the PBS

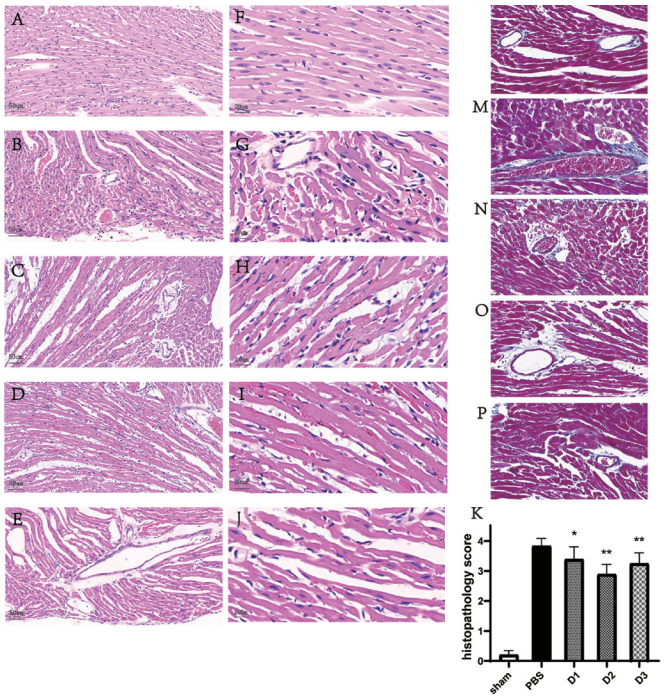

Figure 2. DADLE of different doses alleviated mouse myocardial pathological injury and fibrosis

(A-E) Typical HE-stained myocardial images in the ischemic region at a low magnification. Scale bars = 50 μm. (F-J) Typical myocardial images at a higher magnification. Scale bars = 20 μm. (L-P) Typical images of Masson staining. Scale bars = 20 μm. (A, F, L) Sham group. (B, G, M) PBS control group. (C, H, N) D1 group. (D, I, O) D2 group. (E, J, P) D3 group. (K) Analysis of histopathology scores. **P*<0.05 vs PBS group. ***P*<0.01 vs PBS group. D1 group: DADLE at 0.25 mg/kg. D2 group: DADLE at 0.5 mg/kg. D3 group: DADLE at 1 mg/kg.

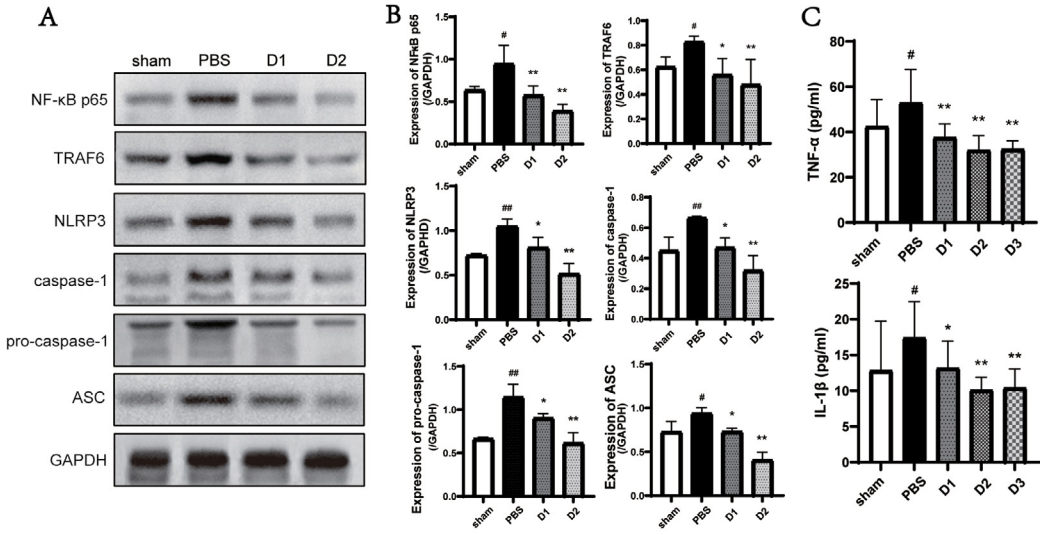

Figure 3. DADLE suppressed protein expressions of the NF-κB/NLRP3 signaling pathway in mice
(A) Expression levels of NF-κB p65, NLRP3, caspase-1, pro-caspase-1, TRAF6, and ASC on Western blot. (B) Quantitative analysis of NF-κB p65, TRAF6, NLRP3, ASC, caspase-1, and pro-caspase-1 expressions. (C) TNF-α and IL-1β levels by ELISA assay. **P*<0.05 vs PBS. ***P*<0.01 vs PBS. #*P*<0.05 vs sham. ##*P*<0.01 vs sham.

control group following I/R (Figure 3C). DADLE at all three dosages significantly reduced the levels of the two mediators (*P*<0.01 or *P*<0.05), especially in the D2 and D3 groups (both *P*<0.01).

DADLE treatment suppressed pyroptosis and apoptosis following MI/R injury

Myocardial pyroptosis was investigated through Western blot and immunofluorescence staining. As indicated in Figure 3, pyroptosis was induced by IRI, evidenced by elevated protein levels of caspase-1, pro-caspase-1, ASC, and NLRP3. Increase in these proteins was partially reversed by DADLE treatment. DADLE at a dosage of 0.5 mg/kg produced a more notable reduction in protein expression than 0.25 mg/kg. ASC, pro-caspase-1, caspase-1, and NLRP3 expression was significantly reduced in both the D1 (*P*<0.05) and the D2 group (*P*<0.01).

Similar to the pyroptosis trend, DADLE mitigated the elevated levels of apoptosis, as demonstrated by TUNEL staining at various doses (Figure 4A-B).

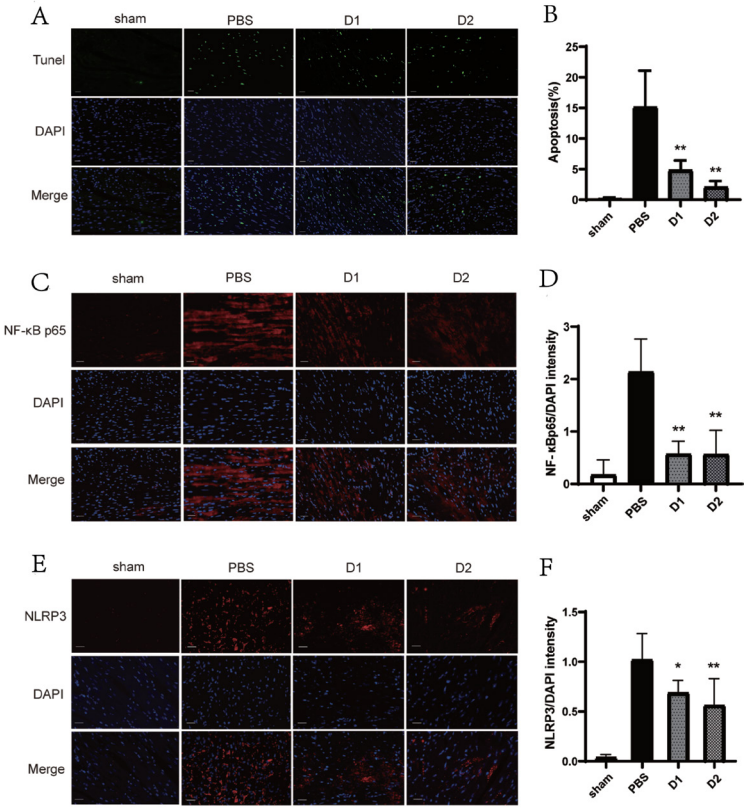

Figure 4. DADLE suppressed apoptosis and pyroptosis following mouse myocardia ischemia-reperfusion injury (MIRI)
(A, B) Typical images and quantification of TUNEL staining. The nuclei of apoptotic cells stained green. Scale bar = 20 μm. (C, E) Typical images of NF-κB p65 and NLRP3 after immunofluorescence staining. (D, F) Quantification of NF-κB p65 and NLRP3 expressions (blue: DAPI; red: NLRP3). **P*<0.05 vs PBS. ***P*<0.01 vs PBS.

Immunofluorescence staining corroborated the western blot findings. Representative images of NF-κB p65 and NLRP3 proteins were shown in Figure 4C and Figure 4E. Quantitative analysis revealed a significant increase in these proteins after I/R, while DADLE at 0.25 and 0.5 mg/kg notably reduced their expression (Figures 4D and 4F).

Discussion

In the present study, DADLE, at different doses, alleviated cardiomyocyte necrosis, fibrosis, and apoptosis as assessed by HE, TTC, Masson, and TUNEL staining. When the DADLE dose was doubled from 0.25 to 0.5 mg/kg, the protective effect was further enhanced. However, at a dosage of 1 mg/kg, the effect diminished. The dose-response trend indicates that neither excessive nor inadequate dosing yields optimal results. This reduction may be linked to an increase in toxic side effects resulting from excessive dosages. These results are consistent with our previous findings **(7)**. In the latter study, DADLE at a dose of 0.5 mg/kg can reduce the area of MI, lower the pathological score, decrease the release of CK-MB and LDH in the myocardium, lower the EF value by cardiac ultrasound, and reduce the expression of caspase-3 protein. Our reperfusion period was set at 24 hr following 45-min ischemia, allowing us to investigate the effects of pharmacological interventions on early cardiac remodeling.

DOR was reported to be present in both animal and human hearts (24, 25). DOR agonists have been shown to provide cardioprotection in animals and in human myocardial cells (26, 27). However, some studies reported conflicting results. For instance, DOR was absent in human and rat engineered myocardial cells (28), and activation of DOR in human atrial cells reduced contractile activity *in vitro* (29).

Several factors may account for these discrepancies. Studies showed that stimulation of DOR in the spinal cord and adrenal glands may exert cardioprotective effects (30), while interactions between DOR and adenosine A1 receptors can enhance the protective effect (31). These complex mechanisms suggest that DOR may function differently *in vivo* compared with *in vitro*. Furthermore, DOR expression may decrease in fibrillating human atria (32) and increase in ventricular myocytes during ischemic events (33), suggesting that DOR distribution in myocardial cells may be uneven and subject to pathological changes. This variability in DOR expression under different conditions may account for the conflicting results, warranting further investigation.

Acute MI triggers an inflammatory response that causes initial myocardial damage. IRI, which occurs when blood flow is restored after MI, leads to a secondary inflammatory storm that exacerbates myocardial injury (34). The inflammatory mechanism plays a central role throughout the MIRI process. During MIRI, NF-κB is indispensable for regulating the transcription of genes encoding inflammatory factors, exemplified by IL-1β and TNF-α (35). These inflammatory mediators continuously activate NF-κB, exacerbating myocardial injury after reperfusion (36, 37). One recent study found that activation of κ-opioid receptors suppresses NF-κB signaling in rat hearts undergoing MI/R (38). Another study by Zhang *et al.* showed that the μ-opioid receptor agonist remifentanil alleviated MIRI via the NF-κB pathway (39). Our study is the first to confirm that the NF-κB signaling pathway mediates the cardioprotective effects of a δ-opioid agonist. Furthermore, our previous research demonstrated that DADLE alleviated cerebral IRI by modulating the TLR4/NF-κB signaling pathway (10). In this study, DADLE significantly reduced NF-κB and inflammatory mediator levels in myocardial cells.

In addition, TRAF6 plays an indispensable role in the NF-κB-mediated inflammatory response (40, 41). TLR4 recruits MyD88, interacts with TRAF6, and transmits signals to activate the NF-κB p65 protein (42). In a study by Meng *et al.* (43), IMTP modified MEs-miR-146a exerted the cardioprotective effect by suppressing the IRAK1/TRAF6/NF-κB signaling pathway. Inhibiting TRAF6 can reduce the activity of the NF-κB pathway, alleviate MIRI, and ameliorate heart failure (44). Our results align with these findings, highlighting the key role TRAF6 plays in DADLE's cardioprotective effects.

NF-κB is directly linked to the regulation of pyroptosis **(45)**. Activation of the NLRP3 inflammasome involves two key processes: firstly, the transcription of the NLRP3 component via the TLR4/NF-κB pathway; and secondly, the assembly of the inflammasome complex, which comprises NLRP3, ASC, and caspase-1. These processes lead to the activation of caspase-1, resulting in the conversion of pro-IL-1β into IL-1β (46). In a study by Hua *et al.* (47), it was shown that the NF-κB/NLRP3/Caspase-1 pathway played a mediating role in cardioprotection after acute MI, improving cardiac functions and alleviating cardiomyocyte injury. Zhang *et al.* (48) reported that diannexin administration modulated TLR4/NF-κB/NLRP3 activation in MI/R mice. Our current findings showed that DADLE alleviated myocardial injury after MIRI through the NF-κB/NLRP3 inflammatory signaling pathway. We presented novel evidence of the involvement of the TRAF6/NF-κB/NLRP3 pathway in MIRI. Interestingly, TUNEL staining revealed that DADLE's inhibitory effect on apoptosis closely mirrored its effect on pyroptosis. DADLE at 0.5 mg/kg demonstrated superior pyroptosis and apoptosis inhibition compared to 0.25 mg/kg.

However, our research also has limitations. First, while the reperfusion time in our experiment was set at 24 hr, extending it to one or two weeks could provide further insights into DADLE's effects on cardiac remodeling. Second, we focused solely on changes in pyroptosis-associated proteins after DADLE administration without exploring protein interrelationships. Future gene knockout experiments are planned to investigate specific roles within the signaling pathway. Additionally, as our experiments were conducted in mice, further studies are required to validate the therapeutic effects and the underlying mechanisms in human cardiomyocytes.

Conclusion

The protective effect of DADLE is dose-dependent, with a dose of 0.5 mg/kg showing the greatest benefit. The TRAF6/NF-κB/NLRP3 signaling pathway may mediate DADLE's protective effects. These lay the foundation for future drug discovery for MIRI.

Acknowledgment

This work was supported by a grant from the Subject Assistance Program of Shanghai Fourth People's Hospital (Grant No. SY-XKZT-2020-1004).

Authors' Contributions

LW L and W C contributed to the conception and

design of the study. LW L collected the data and drafted the manuscript. LW L and YW S constructed the animal model and conducted partial experiments. YY W contributed to data analysis and interpretation. Y W participated in various experiments and assisted in data analysis. W C revised the manuscript and gave\ final approval of the version to be published.

Conflicts of Interest

The authors declare no competing interests.

Declaration

We have not used any AI tools or technologies to prepare this manuscript.

References

1. Wang X, Chen T, Chen S, Zhang J, Cai L, Liu C, *et al.* STING aggravates ferroptosis-dependent myocardial ischemia-reperfusion injury by targeting GPX4 for autophagic degradation. Signal Transduct Target Ther 2025;10:136-152.
2. Martin SS, Aday AW, Almarzooq ZI, Anderson CAM, Arora P, Avery CL, *et al.* 2024 heart disease and stroke statistics: A report of US and Global data from the American Heart Association. Circulation 2024;149:e347-e913.
3. Chen DX, Feng YY, Wang HY, Lu CH, Liu DZ, Gong C, *et al.* Metrnl ameliorates myocardial ischemia-reperfusion injury by activating AMPK-mediated M2 macrophage polarization. Mol Med 2025;31:98-113.
4. Xiang Q, Yi X, Zhu XH, Wei X, Jiang DS. Regulated cell death in myocardial ischemia-reperfusion injury. Trends Endocrinol Metab 2024;35:219-234.
5. Spodnick MB, McElderry SC, Diaz MR. Opioid receptor signaling throughout ontogeny: Shaping neural and behavioral trajectories. Neurosci Biobehav Rev 2025;170:106033.
6. Chen Y, Zhang H, Jiang L, Cai W, Kuang J, Geng Y, *et al.* DADLE promotes motor function recovery by inhibiting cytosolic phospholipase A(2) mediated lysosomal membrane permeabilization after spinal cord injury. Br J Pharmacol 2024;181:712-734.
7. Liu L, Sun Y, Wang Y, Xin J, Chen W. (D-Ala2, D-Leu5)-enkephalin (DADLE) provides protection against myocardial ischemia reperfusion injury by inhibiting Wnt/β-Catenin pathway. BMC Cardiovasc Disord 2024;24:115-125.
8. Xu Y, Chen R, Zhi F, Sheng S, Khiati L, Yang Y, *et al.* δ-opioid receptor, microglia and neuroinflammation. Aging Dis 2023;14:778-793.
9. Zhang S, Yan F, Luan F, Chai Y, Li N, Wang YW, *et al.* The pathological mechanisms and potential therapeutic drugs for myocardial ischemia reperfusion injury. Phytomedicine 2024;129:155649.
10. Fu D, Liu H, Zhu J, Xu H, Yao J. (D-Ala(2), D-Leu(5)) enkephalin inhibits TLR4/NF-κB signaling pathway and protects rat brains against focal ischemia-reperfusion injury. Mediators Inflamm 2021;2021:6661620.
11. Li B, Yang WW, Yao BC, Chen QL, Zhao LL, Song YQ, *et al.* Liriodendrin alleviates myocardial ischemiareperfusion injury via partially attenuating apoptosis, inflammation and mitochondria damage in rats. Int J Mol Med 2025;55:65-76.
12. Zi C, Ma X, Zheng M, Zhu Y. VDAC1-NF-κB/p65-mediated S100A16 contributes to myocardial ischemia/reperfusion injury by regulating oxidative stress and inflammatory response via calmodulin/CaMKK2/AMPK pathway. Eur J Pharmacol 2025;987:177158.
13. Li J, Wei JJ, Wu CH, Zou T, Zhao H, Huo TQ, *et al.* Epimedin A inhibits the PI3K/AKT/NF-κB signalling axis and osteoclast differentiation by negatively regulating TRAF6 expression. Mol Med 2024;30:125-136.
14. Passos PRC, Vieira AA, de Melo RPM, Pinheiro Filho RF, Sampaio LG, Santos H, *et al.* Clustering based on innate immunity reveals differential dysregulation based on disease severity in myelodysplastic neoplasms. Hematol Oncol 2025;43:e70104.
15. Chen XZ, Xu HF, Zhao XM, Li FH, Ren JH, Zhou LY, *et al.* PYRCR alleviates myocardial ischemia/reperfusion injury in mice via inhibiting DRG2-mediated cardiomyocyte pyroptosis. Acta Pharmacol Sin 2025; doi: 10.1038/s41401-025-01604-9.
16. Xu G, Sun X, An J, Sun F, Zhang C, Williams JP. Ozone protects from myocardial ischemia-reperfusion injury via inhibition of the NLRP3 inflammasome. Eur J Pharmacol 2025;997:177631.
17. Pandey A, Li Z, Gautam M, Ghosh A, Man SM. Molecular mechanisms of emerging inflammasome complexes and their activation and signaling in inflammation and pyroptosis. Immunol Rev 2025;329:e13406.
18. Yang Y, Zhu Y, Liu C, Cheng J, He F. Taohong Siwu decoction reduces acute myocardial ischemia-reperfusion injury by promoting autophagy to inhibit pyroptosis. J Ethnopharmacol 2024; 321:117515.
19. Li Y, Wang X, Meng X, Xia C, Yang C, Wang J, *et al.* Aerobic exercise inhibits GSDME-dependent myocardial cell pyroptosis to protect ischemia-reperfusion injury. Mol Med 2024;30:273-284.
20. Ye B, Xu D, Zhong L, Wang Y, Wang W, Xu H, *et al.* Ubiquitin-specific protease 25 improves myocardial ischemia-reperfusion injury by deubiquitinating NLRP3 and negatively regulating NLRP3 inflammasome activity in cardiomyocytes. Clin Transl Med 2025;15:e70243.
21. Liu Y, Li X, Sun T, Li T, Li Q. Pyroptosis in myocardial ischemia/reperfusion and its therapeutic implications. Eur J Pharmacol 2024;971:176464.
22. Gao E, Lei YH, Shang X, Huang ZM, Zuo L, Boucher M, *et al.* A novel and efficient model of coronary artery ligation and myocardial infarction in the mouse. Circ Res 2010;107:1445-1453.
23. Wang D, Wang J, Yang L, Wang X, Huang S. Dexmedetomidine plays a protective role in sepsis-associated myocardial injury by repressing PRMT5-mediated ferroptosis. Toxicol Res (Camb) 2025;14:tfaf010.
24. Theisen MM, Schlottmann S, August C, Herzog C, Theilmeier G, Maas M, *et al.* Detection and distribution of opioid peptide receptors in porcine myocardial tissue. Pharmacol Res 2014;84:45-49.
25. Peng J, Sarkar S, Chang SL. Opioid receptor expression in human brain and peripheral tissues using absolute quantitative real-time RT-PCR. Drug Alcohol Depend 2012;124:223-228.
26. Popov SV, Mukhomedzyanov AV, Maslov LN, Naryzhnaya NV, Kurbatov BK, Prasad NR, *et al.* The infarct-reducing effect of the δ(2) opioid receptor agonist deltorphin II: The molecular mechanism. Membranes (Basel) 2023;13: 63-73.
27. Bell SP, Sack MN, Patel A, Opie LH, Yellon DM. Delta opioid receptor stimulation mimics ischemic preconditioning in human heart muscle. J Am Coll Cardiol 2000;36:2296-2302.
28. Funcke S, Werner TR, Hein M, Ulmer BM, Hansen A, Eschenhagen T, *et al.* Effects of the delta opioid receptor agonist DADLE in a novel hypoxia-reoxygenation model on human and rat-engineered heart tissue: A pilot study. Biomolecules 2020;10:1309-1322.
29. Kunecki M, Płazak W, Roleder T, Biernat J, Oleksy T, Podolec P, *et al.* 'Opioidergic postconditioning' of heart muscle during ischemia/reperfusion injury. Cardiol J 2017;24:419-26.
30. Zhang Y, Irwin MG, Lu Y, Mei B, Zuo YM, Chen ZW, *et al.* Intracerebroventricular administration of morphine confers remote cardioprotection--role of opioid receptors and calmodulin. Eur J Pharmacol 2011;656:74-80.
31. Surendra H, Diaz RJ, Harvey K, Tropak M, Callahan J, Hinek A, *et al.* Interaction of δ and κ opioid receptors with adenosine A1 receptors mediates cardioprotection by remote ischemic preconditioning. J Mol Cell Cardiol 2013;60:142-150.
32. Lendeckel U, Müller C, Röcken C, Laube B, Täger M, Huth C, *et al.* Expression of opioid receptor subtypes and their ligands in fibrillating human atria. Pacing Clin Electrophysiol 2005;28 Suppl 1:S275-S279.
33. Karlsson LO, Bergh N, Li L, Bissessar E, Bobrova I, Gross GJ,

et al. Dose-dependent cardioprotection of enkephalin analogue Eribis peptide 94 and cardiac expression of opioid receptors in a porcine model of ischaemia and reperfusion. Eur J Pharmacol 2012;674:378-383.
34. Dong X, Jiang J, Lin Z, Wen R, Zou L, Luo T, *et al*. Nuanxinkang protects against ischemia/reperfusion-induced heart failure through regulating IKKβ/IκBα/NF-κB-mediated macrophage polarization. Phytomedicine 2022;101:154093.
35. Tian K, Song L, Liu L, Lai T, Liu W. Rutin protects myocardial ischemia-reperfusion injury via the NF-κB/NLRP3/pyroptosis pathway. ACS Omega 2025;10:21777-21785.
36. Ghanta SN, Kattamuri LPV, Odueke A, Mehta JL. Molecular insights into ischemia-reperfusion injury in coronary artery disease: mechanisms and therapeutic implications: A comprehensive review. Antioxidants (Basel) 2025;14: 213-228.
37. Liu X, Shui G, Wang Y, Chen T, Zhang P, Liu L, *et al*. Remimazolam alleviates myocardial ischemia/reperfusion injury and inflammation via inhibition of the NLRP3/IL1β pathway in mice. Int J Mol Med 2025;55: 57-68.
38. Liu H, Huang R, Zhuo Z, Zhang X, Wu L, Guo Z, *et al*. Activation of kappa opioid receptor suppresses post-traumatic osteoarthritis via sequestering STAT3 on the plasma membrane. Cell Commun Signal 2024;22:335-348.
39. Zhang D, Wang Q, Qiu X, Chen Y, Yang X, Guan Y. Remifentanil protects heart from myocardial ischaemia/reperfusion (I/R) injury via miR-206-3p/TLR4/NF-κB signalling axis. J Pharm Pharmacol 2022;74:282-291.
40. Chang W, Chen X, Yang Y, Deng Y, Dong L, Wu H. Geomagnetic activity affects animal myocardial ischemia/reperfusion injury: An experimental-simulated study. Int J Biometeorol 2024;68:731-742.
41. Wu PX, Yang WP, Feng T, Zhang J, Zhu GQ, Du XG, *et al*. African swine fever virus I177L induces host inflammatory responses by facilitating the TRAF6-TAK1 axis and NLRP3 inflammasome assembly. J Virol 2025;99:e0208024.
42. Zhao Z, Li Y, Chi F, Ma L, Li Y, Hou Z, *et al*. Sevoflurane postconditioning ameliorates cerebral ischemia-reperfusion injury in rats via TLR4/MyD88/TRAF6 signaling pathway. Aging (Albany NY) 2022;14:10153-10170.
43. Meng WT, Zhu J, Wang YC, Shao CL, Li XY, Lu PP, *et al*. Targeting delivery of miR-146a via IMTP modified milk exosomes exerted cardioprotective effects by inhibiting NF-κB signaling pathway after myocardial ischemia-reperfusion injury. J Nanobiotechnology 2024;22:382-400.
44. Dawuti A, Sun S, Wang R, Gong D, Liu R, Kong D, *et al*. Salvianolic acid A alleviates heart failure with preserved ejection fraction via regulating TLR/Myd88/TRAF/NF-κB and p38MAPK/CREB signaling pathways. Biomed Pharmacother 2023;168:115837.
45. Bhardwaj A, Panepinto MC, Ueberheide B, Neel BG. A mechanism for hypoxia-induced inflammatory cell death in cancer. Nature 2025;637:470-477.
46. Newton K, Strasser A, Kayagaki N, Dixit VM. Cell death. Cell 2024;187:235-256.
47. Hua F, Li JY, Zhang M, Zhou P, Wang L, Ling TJ, *et al*. Kaempferol-3-O-rutinoside exerts cardioprotective effects through NF-κB/NLRP3/Caspase-1 pathway in ventricular remodeling after acute myocardial infarction. J Food Biochem 2022;46:e14305.
48. Zhang L, Zhao S, Wang Y. Diannexin alleviates myocardial ischemia-reperfusion injury by orchestrating cardiomyocyte oxidative damage, macrophage polarization and fibrotic process by TLR4-NF-kB-mediated inactivation of NLRP3 inflammasome. Int Immunopharmacol 2024;130:111668.